EEP-Vol. 18

APPLICATION OF CAE/CAD TO ELECTRONIC SYSTEMS

presented at

THE 1996 ASME INTERNATIONAL MECHANICAL ENGINEERING CONGRESS AND EXPOSITION
NOVEMBER 17– 22, 1996
ATLANTA, GEORGIA

sponsored by

THE ELECTRICAL AND ELECTRONIC PACKAGING DIVISION, ASME

edited by

DEREJE AGONAFER
IBM CORPORATION

ROBERT E. FULTON
GEORGIA TECH

GREGORY J. KOWALSKI
NORTHEASTERN UNIVERSITY

PETE CIEKURS
NORDEN SYSTEMS

THE AMERICAN SOCIETY OF MECHANICAL ENGINEERS
United Engineering Center / 345 East 47th Street / New York, N.Y. 10017

EEP-Vol. 18, Application of CAE/CAD Electronic Systems
ASME 1996

DETERMINATION OF TEMPERATURES AND HEAT FLUXES ON SURFACES OF MULTI-DOMAIN THREE-DIMENSIONAL ELECTRONIC COMPONENTS

Thomas J. Martin
Department of Aerospace Engineering
The Pennsylvania State University
University Park, PA 16802

George S. Dulikravich
Department of Aerospace Engineering
The Pennsylvania State University
University Park, PA 16802

SUMMARY

A new algorithm that uses the boundary element method (BEM) has been developed for determining steady thermal boundary conditions on surfaces of three-dimensional solids where such quantities are unknown. Given temperature and heat flux on surfaces where such data is readily available, the algorithm computes, non-iteratively, the temperature field within the entire object and any unknown thermal boundary conditions on the surfaces where thermal boundary values are unavailable. An inverse BEM computer program has been developed and was successfully tested on several simple geometries where the analytic solutions of the well-posed problem were known. Our non-iterative algorithm for inverse determination of unknown thermal boundary conditions is very fast and highly flexible in treating complex three-dimensional geometries including interior cavities, mixed thermal boundary conditions and multiple domains with different thermal properties. Besides surface input data, this algorithm accepts also temperatures and heat fluxes at isolated interior points as input data.

INTRODUCTION

Internal heat generation within computer processors increases proportionally to the clock speed of the chip. It is expected that volumetric heat generation inside the new chips will exceed 10×10^{6} W m^{-3} (Bar-Cohen, 1993). In order to monitor the temperature field inside the chip, it would be desirable to place a number of temperature probes as close to the chip as possible. This is impossible to achieve for a number of reasons. First, the temperature probes are electrically operated and could interfere with the electromagnetic field of the chip. Second, since a large number of probes would have to be used, their cost would be significant. Also, although each probe is relatively small, the volume of a large number of probes as compared to a chip and its surrounding is significant. Finally, it is very difficult and practically impossible to place sensors and take measurements of temperatures and heat fluxes on certain surfaces of a heat conducting solid due to the geometric inaccessibility of the surfaces or sensitivity of the environment on these surfaces. Nevertheless, these unknown thermal boundary values may be deduced from additional temperature and heat flux measurements made on some other surfaces. Although the problem is steady state, it has traditionally been solved by resorting to an unsteady heat conduction model (Beck et al., 1985). A characteristic of most of these unsteady inverse techniques is that they produce temporal oscillations in the estimates of the unknown surface thermal conditions that are larger than the temporal oscillations in the over-specified thermal data (Hensel and Hills, 1986). In order to damp out these oscillations, regularization schemes and mollification techniques are employed to smooth the unknown heat fluxes.

Our method (Martin and Dulikravich, 1993; 1994a; 1994b; 1995a; 1995b; 1996; Dulikravich and Martin, 1994a; 1996) for determining the unknown steady boundary conditions does not need any artificial smoothing technique since it is not iterative and has been shown to compute meaningful and accurate thermal fields in a single matrix inversion using a modification to the standard boundary element method (BEM) analysis code. It should be pointed out that this inverse boundary condition method has nothing to do with the inverse domain shaping method (Dulikravich and Martin, 1994b).

BOUNDARY ELEMENT FORMULATION

The governing partial differential equation for steady-state heat conduction in a three-dimensional solid with a constant coefficient of thermal conductivity, and arbitrarily distributed heat sources or sinks per unit volume is

$$k\nabla^2 T(\mathbf{x}) + g(\mathbf{x}) = 0 \qquad (1)$$

where k, T, $\mathbf{x}$ and g are heat conductivity coefficient, temperature, spatial position vector and internal heat source function, respectively. This elliptic partial differential equation can be subject to the Dirichlet (temperature) boundary conditions on the boundary Γ_1, $T = \overline{T}$, the Neumann (heat flux) boundary conditions on the boundary Γ_2, $-k\frac{\partial T}{\partial n} = \overline{Q}$, and, when a boundary is exposed to a moving fluid, the Robin (convective heat transfer) boundary conditions on the boundary Γ_3, $-k\frac{\partial T}{\partial n} = h(T - T_{amb})$. When an ill-posed boundary condition problem is encountered, the boundary Γ_4 has both temperature and heat flux specified and is referred to as an over-specified boundary. At the same time nothing is known on boundary Γ_5. On interface surfaces between domains made of different materials, temperatures and heat fluxes must be the same. Equation (1) can be nondimensionalized using

$$u = \frac{T - T_{min}}{(T_{max} - T_{min})} \qquad b = \frac{gl^2}{k(T_{max} - T_{min})} \qquad (2)$$

where l is the characteristic length scale and u is the non-dimensional temperature so that the non-dimensional heat flux is defined as $q = \frac{\partial u}{\partial n}$. When equation (2) is formulated numerically, an approximate solution, must be used. Therefore, error, often called the residual, is introduced into problem. The weighted residual statement minimizes this error by setting the weighted sum of the residuals over the entire domain and in the boundary conditions to zero. For Poisson's equation, the weighted residual statement appears as

$$\int_\Omega \left(\nabla^2 u(\mathbf{y}) + b(\mathbf{y})\right) w(\mathbf{x},\mathbf{y})\, d\Omega(\mathbf{y}) + \int_{\Gamma_1} \left(u(\mathbf{y}) - \overline{u}(\mathbf{y})\right) \frac{\partial w(\mathbf{x},\mathbf{y})}{\partial n}\, d\Gamma(\mathbf{y}) - \int_{\Gamma_2} \left(q(\mathbf{y}) - \overline{q}(\mathbf{y})\right) w(\mathbf{x},\mathbf{y})\, d\Gamma(\mathbf{y}) = 0 \qquad (3)$$

The fundamental Green's function solution, which will be represented by u*, replaces the weighting function, w. It satisfies the following Green's function solution equation with a unit impulsive heat source and homogeneous boundary conditions.

$$\nabla^2 u^* + \delta(\mathbf{x} - \mathbf{y}) = 0 \qquad (4)$$

The Dirac delta function, $\delta(\mathbf{x}\text{-}\mathbf{y})$, has the following sifting property.

$$\int_\Omega f(\mathbf{y})\delta(\mathbf{x} - \mathbf{y})\, d\Omega = \begin{cases} 0 & \text{when x is outside } \Omega \\ f(\mathbf{x}) & \text{when x is inside } \Omega \end{cases} \qquad (5)$$

After integrating the weighted residual statement (Eq. 3) by parts twice, retaining the Cauchy principal value of the boundary integrals, and using the properties of the Dirac delta function , the following Boundary Integral Equation (BIE) is obtained (Brebbia, 1978)

$$c(\mathbf{x})u(\mathbf{x}) + \int_\Gamma q^*(\mathbf{x},\mathbf{y})\, u(\mathbf{y})\, d\Gamma = \int_\Gamma u^*(\mathbf{x},\mathbf{y})\, q(\mathbf{y})\, d\Gamma + \int_\Omega u^*(\mathbf{x},\mathbf{y})\, b(\mathbf{y})\, d\Omega \qquad (6)$$

The boundary integral is singular where the observation point, $\mathbf{x}$, is on the boundary. These singular integrals must be evaluated in the sense of the Cauchy principal value (Brebbia, 1978). Consequently, $c(\mathbf{x}) = 0.0$ when $\mathbf{x}$ is outside the domain, $c(\mathbf{x}) = 1.0$ when $\mathbf{x}$ is inside the domain and $c(\mathbf{x}) = \theta/4\pi$ when $\mathbf{x}$ is on the boundary, where θ is the internal angle at the corner between two neighboring boundary elements. If the temperature gradient is known at some location in the domain, the following BIE can be derived (Brebbia, 1978)

$$\nabla u(\mathbf{x}) + \int_\Gamma \nabla q^*(\mathbf{x},\mathbf{y})\, u(\mathbf{y})\, d\Gamma = \int_\Gamma \nabla u^*(\mathbf{x},\mathbf{y})\, q(\mathbf{y})\, d\Gamma + \int_\Omega \nabla u^*(\mathbf{x},\mathbf{y})\, b(\mathbf{y})\, d\Omega \qquad (7)$$

The fundamental solution for the three-dimensional Poisson equation is

$$u^* = \frac{1}{4\pi|\mathbf{x} - \mathbf{y}|} \qquad (8)$$

The boundary was discretized into N bilinear, isoparametric, boundary elements connected at N boundary node resulting in a set of N boundary integral equations. Only this portion of the domain, Ω, that contains heat sources was discretized into N_{VC} isoparametric trilinear cells sharing both domain and boundary nodes in order to evaluate the field source

integral. Since the unknowns existed only on the boundary, the set of BIE's was arranged into the following matrix form, with the geometric coefficients matrices [H], [G] and [P] computed by integrating the fundamental solution distributed on the boundary and in the domain.

$$[\mathbf{H}]\{\mathbf{U}\} = [\mathbf{G}]\{\mathbf{Q}\} + [\mathbf{P}]\{\mathbf{B}\} \tag{9}$$

For a well-posed boundary value problem, every point on the boundary is given one Dirichlet, Neumann or Robin-type boundary condition, no internal temperature measurements exist, and the heat source vector {B} is entirely known. Once the boundary conditions are multiplied out, they can be collected on the right hand side and added to [P]{B} to form a vector of knowns, {F}. The left-hand side will remain in the standard form [A]{X}, having N unknowns and N equations. This system of linear algebraic equations can be solved for the unknowns on the boundary by any standard matrix solver such as Gaussian elimination or LU factorization.

If the boundary conditions in the above example are not properly applied, or if internal temperature measurements are included in the analysis, or if part or all of the heat source function is unknown, the problem becomes ill-posed. A solution may still be obtained by multiplying the known quantities in the vectors {U}, {Q} and {B} by their respective coefficient matrix columns and collecting them into the vector of knowns. The unknowns form a single vector, {X}, multiplied by a highly ill-conditioned coefficient matrix, [A], which is, in general, not square (Martin and Dulikravich, 1996; Dulikravich and Martin, 1996).

SINGULAR VALUE DECOMPOSITION

Such matrices can be inverted using Singular Value Decomposition (SVD) methods (Beck et al., 1985; Press et al., 1992; Throne and Olson, 1994; Pawluk, 1995). The goal of the SVD is to choose a solution vector {X} so as to minimize the error

$$E = \|\{\mathbf{F}\} - [\mathbf{A}]\{\mathbf{X}\}\| \tag{10}$$

Any M x N matrix [A] can be written as the product of an M x N column-orthogonal matrix, [C], an N x N diagonal matrix [S] with positive singular values, and the transpose of an N x N orthogonal matrix [D].

$$[\mathbf{A}] = [\mathbf{C}] \begin{bmatrix} s_1 & 0 & 0 \\ 0 & 0 & 0 \\ 0 & 0 & s_N \end{bmatrix} [\mathbf{D}] \tag{11}$$

The singular values, $s_1, s_2, \ldots, s_N$, are the eigenvalues of a matrix $[\mathbf{A}]^T[\mathbf{A}]$. Formally, the condition number of a matrix is defined as the ratio of the largest of the s_j's to the smallest of the s_j's. For a well-conditioned matrix, these values will be roughly of the same order of magnitude. As the matrix becomes more ill-conditioned, these values become more dispersed. If the matrix [A] is singular, then there is some subspace of {X}, called the nullspace, that is mapped to zero, that is, [A]{X}={0}. The LU factorization and Gaussian elimination techniques may give a formal solution to an ill-conditioned set of equations, but the solution vector {X} will have highly oscillating components. When this solution vector, {X}, is multiplied by the matrix [A], a very poor approximation to the vector {F} will be the result. Eliminating very small singular values has the effect of removing those algebraic terms that, because they are dominated by noise and round-off error, corrupt the solution. In order to determine which singular values are to be truncated, we must choose a singularity threshold parameter, τ, so that if $s_j/s_{max} < \tau$, then $1/s_j = 0$. Since [C] and [D] are each orthogonal in the sense that their columns are orthonormal, the solution vector can be easily found as

$$\{\mathbf{X}\} = [\mathbf{D}][\mathrm{diag}(1/s_j)]\left([\mathbf{C}]^T\{\mathbf{F}\}\right) \tag{12}$$

VERIFICATION OF ACCURACY OF THE ANALYSIS AND INVERSE BEM COMPUTER CODES

A BEM computer program was developed using the theory discussed in the previous section. The accuracy of the three-dimensional BEM as a solution to the well-posed heat conduction problem was verified for the test case consisting of an unit size cube centered at (0, 0, 0) with a centrally located cubical cavity of the size 0.4m x 0.4m x 0.4m. All six walls of the cubical cavity were at T = 100 K. Outside surface of the cube was assigned the following boundary conditions: front and back walls were adiabatic, while left and right vertical walls and the top and bottom walls were at T = 1000 K. Since a closed-form analytic solution cannot be found for this test case, we utilized a second-order accurate alternating-direction implicit finite difference algorithm (Dennis, 1996) to obtain an accurate thermal field prediction for this well-posed problem. When using the finite difference analysis code and the BEM analysis code we discretized the cube with 25 x 25 x 25 uniform grid cells and the cavity with 5 x 5 x 5 uniform grid cells. Compared with the finite difference solution, the BEM analysis code had maximum local relative error of 0.2% in predicted heat fluxes on the front and back outer walls and 0.5% in predicted heat fluxes normal to the cavity walls. The SVD threshold parameter used in the well-posed problem solution was of the order of $\tau = 10^{-6}$.

An ill-posed problem was then created by treating all six walls of the cubical cavity as thermally unspecified, that is, as if we do not know temperatures and heat fluxes on these surfaces. At the same time, we enforced T = 1000 K on all six outside walls and adiabatic conditions on the outer front and back walls thus making them the over-specified boundaries. Our inverse BEM code solved this ill-posed problem resulting in an average 5% error in the predicted cavity surface temperatures and 8% error in the predicted cavity surface heat fluxes (Figure 1). The errors were concentrated at the corners of the cubic cavity. The SVD threshold parameter used in the ill-posed problem

solution was of the order of $\tau = 10^{-2}$ (Martin and Dulikravich, 1996).

THERMAL ANALYSIS OF A COOLED MODEL MULTIDOMAIN ELECTRONIC CHIP PACKAGE

For the purpose of demonstrating the flexibility of our BEM code to treat three-dimensional configurations composed of subdomains having different thermal properties and different geometries, we have created a simplified cooled chip package configuration (Figure 2). It consists of a tungsten ($k = 137$ W m^{-1} K^{-1}) heat sink with four vertical parallel plate-fins (Figure 3), a square heat spreader plate (Figure 4) made of silica with $k = 1.39$ W m^{-1} K^{-1}, a square substrate plate (Figures 5 and 6) made of SiO_2 with $k = 1.39$ W m^{-1} K^{-1} (Yamaguchi et al., 1992), and a square chip (Figure 7) made of Si with $k = 102$ W m^{-1} K^{-1} (Yamaguchi et al., 1992). The relative dimensions can be discerned from the scales indicated in Figure 2. Specifically, the chip measured 15 mm x 15 mm. It was imbedded in a square SiO_2 substrate plate measuring 35 mm x 35 mm. It should be pointed out that this is not a realistic configuration (Shaukatullah and Gaynes, 1995), but strictly a simplified and a fictitious configuration that will be analyzed only for the purpose of a preliminary demonstration of the versatility, speed and accuracy of our analysis and inverse boundary condition determination methodology.

First, a well-posed analysis problem was formulated by specifying convective heat transfer coefficient $h = 3000$ W m^{-2} K^{-1} on the surfaces of all the plate-fins, while the remaining exterior surfaces of the assembled configuration were treated as adiabatic (Figure 2). Ambient fluid temperature was specified as $T_{amb} = 300$ K. Nothing was specified on the surface of the chip and on the interface (contact) surfaces of the other components. There, interface compatibility conditions (equal temperatures and heat fluxes from both sides of the interface) were automatically enforced.

Our BEM analysis code generated surface grids (Figures 3-7) that resulted in a system of 740 algebraic equations for the unknown surface temperatures and heat fluxes. On a Cray C-90 computer with a single vector processor it took 1.5 seconds to form the solution matrices and an additional 11 seconds to solve them using SVD algorithm. Our code is very fast due to the fact that it is fully vectorized and does not need any iterative procedures since it is based on BEM. Details of the predicted temperatures on the surfaces of each of the components are depicted in Figures 3-7. It can be seen that the tips of the heat sink fins are practically useless (Figure 3) suggesting that the fins could be shortened. The isotherm pattern on the top surface of the heat spreader plate is practically constant (Figure 4) although the chip below acts as a square source of heat. Similar conclusion can be drawn concerning the substrate plate (Figures 5 and 6). With the present configuration and chosen thermal conductivities of the package components, the chip itself has a mildly non-uniform temperature distribution (Figure 7). Notice that Figure 7 is not drawn to scale.

This analysis strongly suggests that more uniform temperature field and lower overall temperature could be achieved in the chip by utilizing a constrained shape inverse design methodology (Dulikravich and Martin, 1994; 1996) and the BEM thermal analysis software.

INVERSE DETERMINATION OF BOUNDARY CONDITIONS ON A COOLED MODEL MULTIDOMAIN ELECTRONIC CHIP PACKAGE

One of the by-products of the well-posed problem solution procedure is the computed temperature distribution on the bottom surface of the substrate plate (Figure 6). Recall that the boundary condition enforced on this bottom surface was zero heat flux (adiabatic wall).

Then, we created an ill-posed (inverse) problem for the same multidomain cooled chip package (Figure 2). The vertical surfaces of the finned heat sink were assigned overspecified thermal boundary conditions consisting of the surface temperatures and heat fluxes computed from the previous well-posed analysis problem. The remaining outer vertical surfaces of the package were assigned adiabatic condition as in the analysis (forward or well-posed) case. Thermal boundary conditions on the entire bottom horizontal surface of the substrate plate were treated as unknown, that is, nothing was specified on the bottom surface of the package. It an actual application of this methodology, the overspecified thermal boundary conditions can be provided from experimentally measured values on any accessible surface. Similarly, any surface or surfaces can be treated as inaccessible where experimental values of temperature and heat fluxes are unavailable.

Our inverse BEM code solved this example ill-posed problem (consisting of 740 equations and 632 unknowns) in the same amount of computer time as it did the previous well-posed problem. The SVD threshold parameter used in the ill-posed problem solution was of the order of $\tau = 10^{-5}$. The temperature field predicted on the surface of the heat spreader plate (Figure 8) was almost identical to the values obtained from the solution of the forward problem (Figure 4). Surface temperature distribution predicted on the interface surface between substrate and the heat spreader plate closely resembled (Figure 9) the values obtained from the solution of the forward problem (Figure 5). Isotherms inversely predicted on the bottom surface of the substrate plate (Figure 10) differed somewhat from the temperature field obtained from the well-posed problem (Figure 6). The relative error was below 10% which can be considered acceptable because a relatively coarse grid was used and the over-specified boundary conditions already contained an error since they were obtained from the numerical solution of the well-posed problem. At the same time, it is remarkable that the inverse BEM predicted a negligibly small value for the heat flux on the bottom surface of the substrate plate where we know that the correct answer is zero heat flux.

Temperatures predicted on the surface of the chip (Figure 11) with our inverse BEM code compared very well with the values predicted using our analysis BEM code (Figure 7). It is especially interesting to note that the maximum relative error in the inversely predicted chip surface temperature was only 0.3%. This suggests that this inverse technique for determining chip surface temperatures and heat fluxes can be used with a great degree of confidence

even in the situation when only a limited amount of combined temperature and heat flux measurements is available on some other more accessible exterior surfaces of the entire 3-D electronic package.

CONCLUSIONS

We have recently developed a three-dimensional version of our inverse method that has the capability to determine thermal boundary conditions (temperatures and heat fluxes) on surfaces of conducting three-dimensional solid objects where such quantities are unknown. The solid can be composed of an arbitrary number of arbitrarily shaped components where each component can be made of a different material. Our method is very fast since it uses a non-iterative direct approach based on boundary integral method in solving steady-state inverse heat conduction problems of unknown boundary condition type. This means that given any over-specified thermal boundary conditions (such as temperatures and heat fluxes on surfaces where such data are readily available) the algorithm is capable of predicting the temperature field within each component. In addition, the algorithm simultaneously predicts all unknown thermal boundary conditions on surfaces of each component where the thermal boundary conditions were not specified. A BEM computer code has been developed to perform automatic non-iterative determination of steady temperatures and heat fluxes on parts of the interior and exterior boundaries of multidomain arbitrarily shaped 3-D solids. Accuracy of the computer code was tested on several simple geometries by comparing the results of the inverse BEM code against the results of a finite difference analysis code. Results were in very good agreement in the regions relatively close to the overspecified data, but deteriorated with the distance from the overspecified boundaries.

ACKNOWLEDGMENTS

Authors would like to express their appreciation for the partial support provided by the NSF Grant DMI-9522854 supervised by Dr. G. A. Hazelrigg. and the ALCOA Research Faculty Fellow Award administered by Dr. Yimin Ruan. Special thanks are due Dr. H. Shaukatullah of IBM, Endicott, NY for useful comments and discussions concerning heat sink parameters.

REFERENCES

Bar-Cohen, A., 1993, "Thermal Management of Electronic Components With Dielectric Liquids," *JSME Internat. Journal, Series B*, Vol. 36, No. 1, pp. 1-25.

Beck, J. V., Blackwell, B. and St. Clair, C. R. Jr., 1985, *Inverse Heat Conduction: Ill-Posed Problems*, Wiley-Interscience, New York..

Brebbia, C. A., 1978, *The Boundary Element Method for Engineers*, John Wiley & Sons, New York.

Dennis, B. H.., 1996, Private Communications, The Pennsylvania State University.

Dulikravich, G. S. and Martin, T. J., 1994a, "Inverse Problems and Design in Heat Conduction", *Proceedings of 2nd International Symposium on Inverse Problems in Engineering*, Nov. 2-4. 1994, Editors: H. D. Bui, M. Tanaka, M. Bonnet, H. Maigre, E. Luzzato and M. Reynier, Paris, France, November 2-4, 1994, A. A. Balkema, Rotterdam, 1994, pp. 13-20.

Dulikravich, G. S. and Martin, T. J., 1994b, "Inverse Design of Super-Elliptic Cooling Passages in Coated Turbine Blade Airfoils", *AIAA Journal of Thermophysics and Heat Transfer*, Vol. 8, No. 2, pp. 288-294.

Dulikravich, G. S. and Martin, T. J., 1996, "Inverse Shape and Boundary Condition Problems and Optimization in Heat Conduction", Chapter no. 10 in *Advances in Numerical Heat Transfer, Vol. 1*, Editors: W. J. Minkowycz and E. M. Sparrow, Taylor and Francis.

Hensel, E. and Hills,, R. G., 1986, "An Initial Value Approach to the Inverse Heat Conduction Problem", *ASME Journal of Heat Transfer*, Vol. 108, pp. 248-256.

Martin, T. J. and Dulikravich, G. S., 1993, "A Direct Approach to Finding Unknown Boundary Conditions in Steady Heat Conduction", *Proceedings of 5th Annual Thermal and Fluids Workshop*, Lewis Research Center, Cleveland, OH, Aug. 1993, NASA CP-10122, pp. 137-149.

Martin, T. J. and Dulikravich, G. S., 1994a, "Inverse Determination of Temperatures and Heat Fluxes on Inaccessible Surfaces", in *Proceedings of BETECH'94*, Orlando, FL, March 16-18, 1994, in *Boundary Element Technology IX*, Computational Mechanics Publications, Southampton, England; Editors: C. A. Brebbia and A. Kassab, pp. 69-76.

Martin, T. J. and Dulikravich, G. S., 1994b, "Finding Unknown Surface Temperatures and Heat Fluxes in Steady Heat Conduction", *Proceedings of 4th InterSociety Conference on Thermal Phenomena in Electronic Systems (ITHERM IV)*, May 4-7, 1984, Washington, D.C., Editors: A. Ortega and D. Agonafer, pp. 214-221; also in *IEEE Transactions of Components, Packaging and Manufacturing Technology (CPMT) Society - Series A*, Vol. 18, No. 3, pp. 540-545, September 1995.

Martin, T. J. and Dulikravich, G. S., 1995a, "Inverse Determination of Boundary Conditions in Steady Heat Conduction With Heat Generation", *Symposiums on Conjugate Heat Transfer, Inverse Problems, and Optimization, and Inverse Problems in Heat Transfer*, Editors: W. J. Bryan and J. V. Beck, ASME National Heat Transfer Conference, Portland, OR, August 6-8, 1995, ASME HTD-Vol. 312, pp. 39-46.

Martin, T. J. and Dulikravich, G. S., 1995b, "Finding Temperatures and Heat Fluxes on Inaccessible Surfaces in 3-D Coated Rocket Nozzles", *Proceedings of 1995 JANNAF Propulsion and Subcommittee Joint Meeting*, Tampa, Florida, December 4-8, 1995.

Martin, T. J. and Dulikravich, G. S., 1996, "Inverse Determination of Boundary Conditions in Steady Heat Conduction with Heat Generation," *ASME Journal of Heat Transf.*, Vol. 118, No. 3, Aug. 1996, pp. 546-554.

Pawluk, K., 1995, Computational Magnetics, Chapter 5, Editor: Sykulski, J. K., Chapman & Hall, London, UK.

Press, W. H., Teukolsky, S. A., Vetterling, W. T. and Flannery, B. P., 1992, *Numerical Recipes in FORTRAN*, Second Edition, Cambridge University Press.

Shaukatullah, H. and Gaynes, M. A., 1995, "Comparative Evaluation of Various Types of Heat Sinks for Thermal Enhancement of Surface Mount Plastic Packages", *Int. J. of Microcircuits and Electronic Packaging*, Vol. 18,

No. 3, 3rd quarter, pp. 252-258.

Throne, R. D. and Olson, L. G., 1994, "A Generalized Eigensystem Approach to the Inverse Problem of Electrocardiography", *IEEE Transact. on Biomedical Engineering*, Vol. 41, No. 6, pp. 1-9, June 1994.

Yamaguchi, H., Hirasawa, S., Owada, N. and Natsuaki, N. 1992, "Analysis of Localized Temperature Distribution in SOI Devices", *IECE Transactions in Electron.*, Vol. E75-C, No. 12, December 1992. pp. 1438-1441.

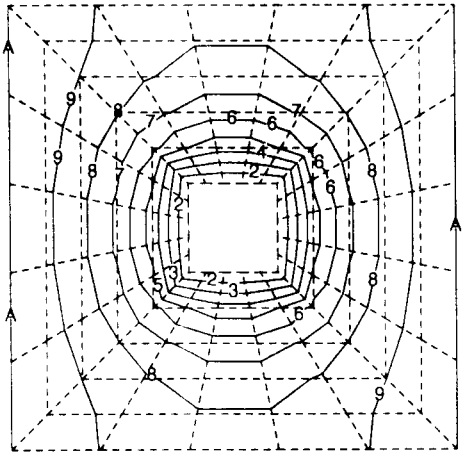

Level	t
A	1000
9	900
8	800
7	700
6	600
5	500
4	400
3	300
2	200
1	100

a)

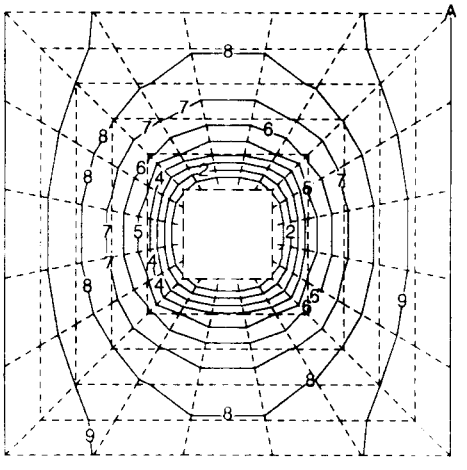

Level	t
A	1000
9	900
8	800
7	700
6	600
5	500
4	400
3	300
2	200
1	100

b)

FIGURE 1 COMPUTED ISOTHERMS (SOLID LINES) ON A SYMMETRY PLANE OF A BOX-IN-A-BOX 3-D CONFIGURATION: A) FORWARD PROBLEM SOLUTION, B) INVERSE PROBLEM SOLUTION AND THE COMPUTATIONAL GRID (DASHED LINES).

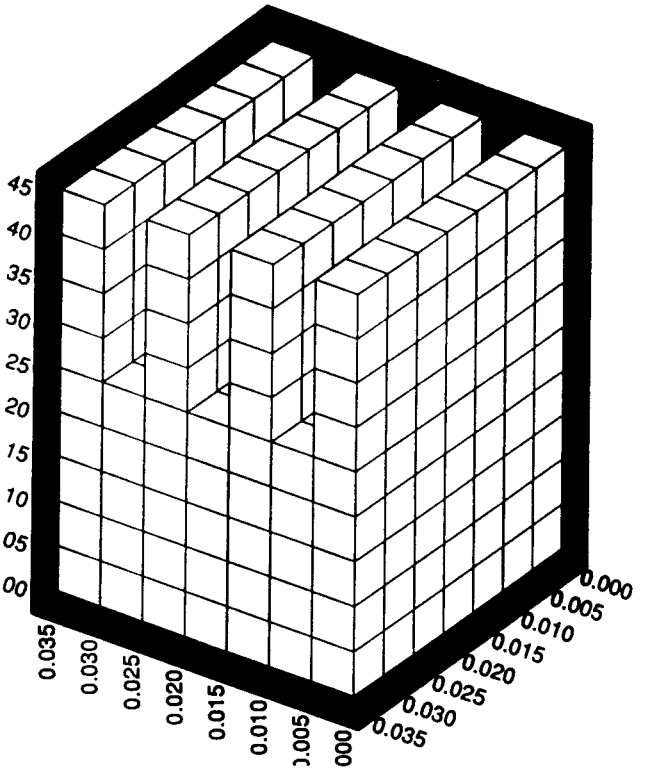

FIGURE 2 COMPUTATIONAL GRID FOR A COOLED CHIP PACKAGE.

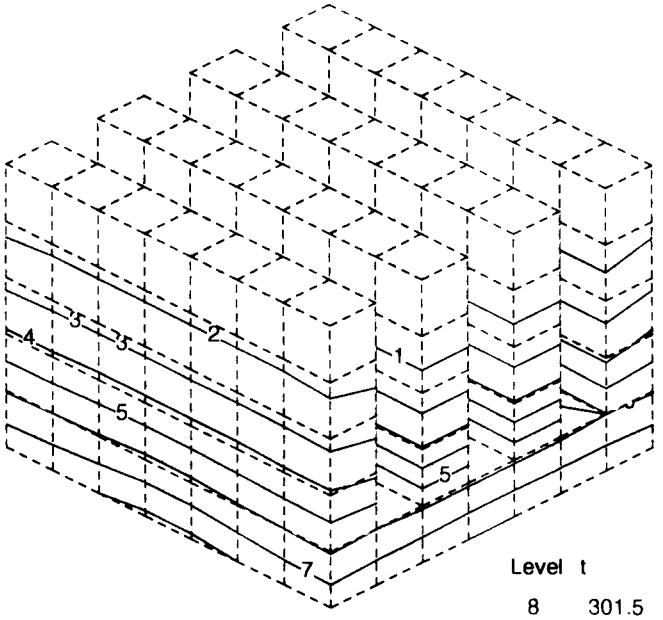

Level	t
8	301.5
7	301.35
6	301.2
5	301.05
4	300.9
3	300.75
2	300.6
1	300.45

FIGURE 3 FORWARD PROBLEM: COMPUTED SURFACE ISOTHERMS (SOLID LINES) AND SURFACE COMPUTATIONAL GRID (DASHED LINES) ON THE FINNED HEAT SINK.

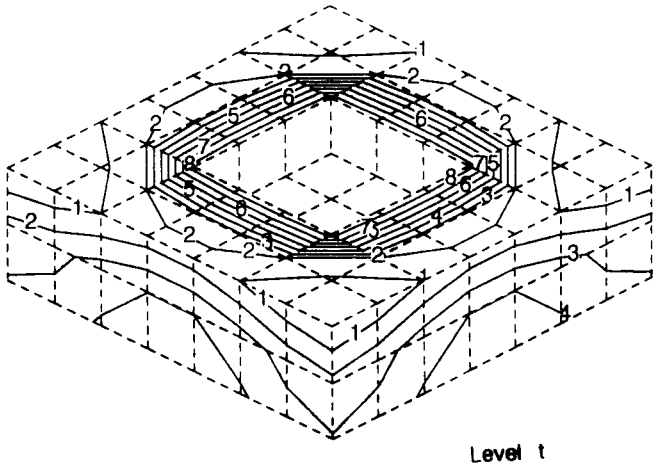

Level	t
8	387.068
7	381.696
6	376.323
5	370.951
4	365.579
3	360.207
2	354.834
1	349.462

FIGURE 5 FORWARD PROBLEM: COMPUTED SURFACE ISOTHERMS (SOLID LINES) AND SURFACE COMPUTATIONAL GRID (DASHED LINES) ON THE UPPER SURFACE OF THE SUBSTRATE PLATE.

Level	t
8	382.073
7	371.996
6	361.92
5	351.843
4	341.767
3	331.69
2	321.614
1	311.537

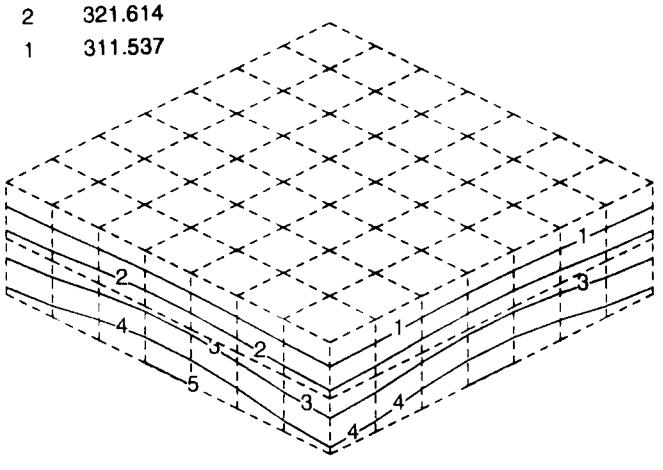

FIGURE 4 FORWARD PROBLEM: COMPUTED SURFACE ISOTHERMS (SOLID LINES) AND SURFACE COMPUTATIONAL GRID (DASHED LINES) ON THE HEAT SPREADER PLATE.

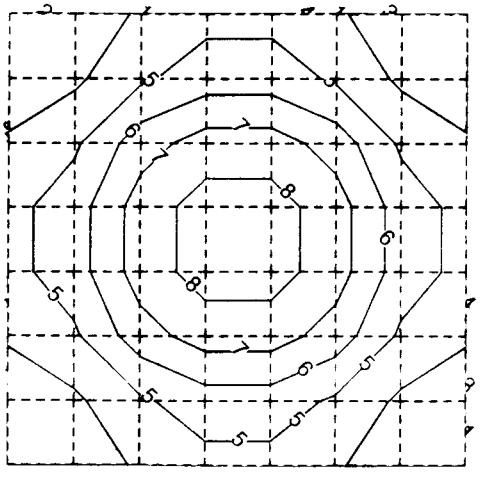

Level	t
8	387.068
7	381.696
6	376.323
5	370.951
4	365.579
3	360.207
2	354.834
1	349.462

FIGURE 6 FORWARD PROBLEM: COMPUTED SURFACE ISOTHERMS (SOLID LINES) AND SURFACE COMPUTATIONAL GRID (DASHED LINES) ON THE BOTTOM SURFACE OF THE SUBSTRATE PLATE.

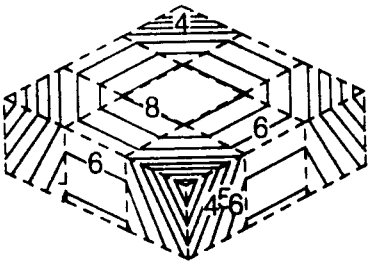

Level	t
8	391.399
7	391.098
6	390.797
5	390.496
4	390.194
3	389.893
2	389.592
1	389.291

FIGURE 7 FORWARD PROBLEM: COMPUTED SURFACE ISOTHERMS (SOLID LINES) AND SURFACE COMPUTATIONAL GRID (DASHED LINES) ON THE SURFACE OF THE CHIP.

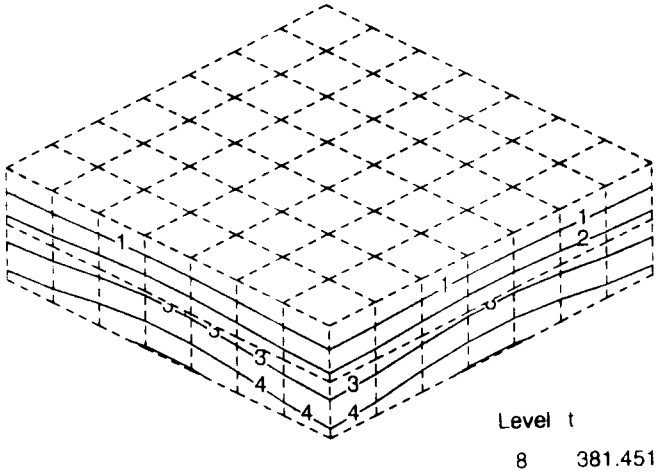

Level	t
8	381.451
7	371.452
6	361.453
5	351.454
4	341.456
3	331.457
2	321.458
1	311.459

FIGURE 8 INVERSE PROBLEM: COMPUTED SURFACE ISOTHERMS (SOLID LINES) AND SURFACE COMPUTATIONAL GRID (DASHED LINES) ON THE HEAT SPREADER PLATE.

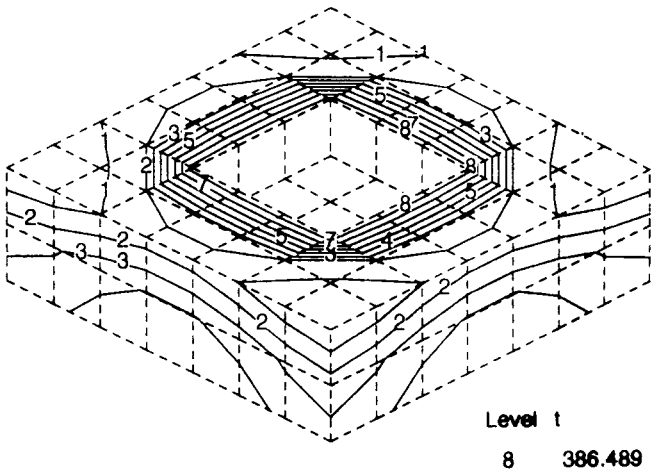

Level	t
8	386.489
7	381.278
6	376.067
5	370.856
4	365.644
3	360.433
2	355.222
1	350.011

FIGURE 9 INVERSE PROBLEM: COMPUTED SURFACE ISOTHERMS (SOLID LINES) AND SURFACE COMPUTATIONAL GRID (DASHED LINES) ON THE UPPER SURFACE OF THE SUBSTRATE PLATE.

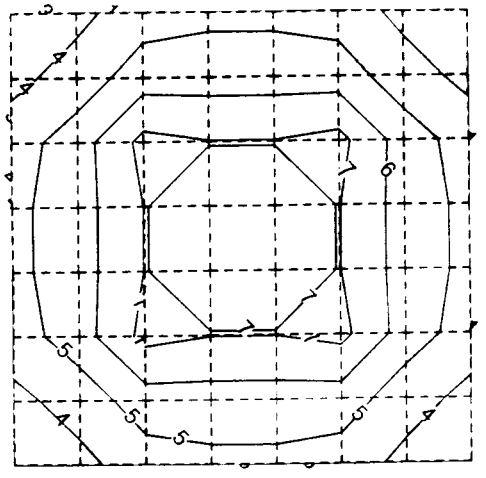

Level	t
8	386.489
7	381.278
6	376.067
5	370.856
4	365.644
3	360.433
2	355.222
1	350.011

FIGURE 10 INVERSE PROBLEM: COMPUTED SURFACE ISOTHERMS (SOLID LINES) AND SURFACE COMPUTATIONAL GRID (DASHED LINES) ON THE BOTTOM SURFACE OF THE SUBSTRATE PLATE.

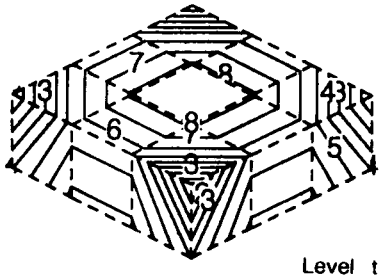

Level	t
8	392.127
7	391.814
6	391.5
5	391.187
4	390.873
3	390.56
2	390.246
1	389.933

FIGURE 11 INVERSE PROBLEM: COMPUTED SURFACE ISOTHERMS (SOLID LINES) AND SURFACE COMPUTATIONAL GRID (DASHED LINES) ON THE SURFACE OF THE CHIP.